On the Adaptation of Dynamic Walking to Persistent External Forcing using Hybrid Zero Dynamics Control

Sushant Veer, Mohamad Shafiee Motahar, and Ioannis Poulakakis

***Abstract*— This paper investigates the ability of dynamically walking bipeds to adapt their motion to persistent exogenous forcing. Applications that involve physical interactions between a bipedal robot and other robots (or humans), require that the robot adjust its stepping pattern in response to externally applied force signals. In our setting, an underactuated bipedal robot model walks under the influence of an external force. First, the hybrid zero dynamics method is used to design controllers that stabilize periodic walking motions in the absence of the external force. Then, conditions are derived analytically under which these (unforced) periodic gaits are modified to new (possibly aperiodic) stepping patterns that are consistent with the external force. It is deduced that underactuation holds the key to the ability of our model to adapt to external forces.**

I. Introduction

Legged locomotion controllers, *particularly* those for dynamically-stable locomotion, focus—almost exclusively—on enhancing the stability and robustness of the resulting motions, typically treating the environment as a source of disturbances that must be rejected. Yet, engaging bipedal robots in tasks that combine locomotion and cooperation with other robots or humans via physical interaction, necessitates that the biped be capable of adapting its locomotion to external forcing. This paper studies the adaptability of dynamically walking bipeds to externally applied forces by interpreting such forces as "command" signals that intend to regulate the biped's motion.

Incorporating external forces in legged locomotion controllers has been studied in the context of quasi-statically moving humanoid robots. Based on the Zero Moment Point (ZMP) criterion of stability, model predictive controllers for push recovery [1], and adaptive foot positioning [2] have been employed to generate stable gaits. Along similar lines, a variety of ZMP-based methods have been proposed to engage humanoids in tasks that involve external forces; the book [3] provides examples of humanoids pushing objects, moving obstacles out of their way, or carrying heavy objects over a distance. *Dynamically-stable* walking bipeds, on the other hand, have not enjoyed the popularity of their quasi-static counterparts in such activities.

A number of methods are available for generating and sustaining periodic walking motions on bipeds. The hybrid zero dynamics (HZD) method [4], and its recent extensions [5], [6], have been successful in experimentally generating and sustaining periodic walking motions on bipeds with point [7], as well as curved [8], feet. Other methods include human-inspired [9], geometric reduction [10], and stochastic control [11], approaches to stabilize dynamic walking on bipedal robots. In nearly all cases, however, the controllers are derived in isolation from exogenous forces. A notable exception to this general rule is [12], which uses the notion of partial hybrid zero dynamics [9] to incorporate interaction forces that are external to the locomotion system, and are generated due to manipulating an object. Again though, the proposed controller is specifically designed so that the interaction forces do *not* interfere with locomotion.

In this paper, we turn our attention to external forces that are applied on a dynamically walking biped *intentionally*, with the purpose of modifying its motion. An instance of this general case has been investigated in [13], in which a human literally "walks" Acroban, a recently developed compliant humanoid robot. As the human moves, it holds the robot, which adapts to the external force by modifying its walking gait accordingly. Similar situations arise in applications where humans and robots cooperate to transport objects over a distance that is large enough to require the use of the locomotion system of the robot [14]. In such cooperative tasks, the robot experiences a persistent external force that differs from disturbances acting momentarily in a fundamental way: the robot should adapt its motion to this force rather than trying to return to its original gait, as is the case in HZD [4], [5], partial HZD [9], or capture point [15] controllers. In the context of dynamically walking bipeds, realizing such human-robot teams requires a deeper understanding of how the underlying locomotion controller reacts to *persistent* external forcing

Motivated by this type of interactions, we analyze the motion of an underactuated bipedal robot model under an exogenous force. To keep the model general, we consider forces that are functions of time satisfying a smoothness assumption. The inclusion of such forces results in a time-varying system, increasing the complexity of the associated analysis. In this setting, utilizing properties of the HZD [4], [16], analytical expressions that capture the step-to-step evolution of the biped's motion under the influence of the external force are obtained. These expressions are then used to derive explicit conditions that couple the state of the robot at the beginning of a step with the force applied over that step to determine whether the model successfully completes the step. It is deduced that, as long as these conditions are satisfied and sufficiently fast convergence to the zero dynamics surface can be achieved, the robot adapts to the external force by altering its stepping frequency without

S. Veer, M. S. Motahar and I. Poulakakis are with the Department of Mechanical Engineering, University of Delaware, Newark, DE 19716, USA; e-mail: {veer, motahar, poulakas}@udel.edu.

This work is supported in part by NSF grant NRI-1327614.

changing its step length. We subsequently apply our analysis to the cases of constant and periodic external force profiles. Interestingly, if under a periodic force the biped converges to a limit cycle, then it can be proved that its period is equal to an integer multiple of the period of the force.

This paper is organized as follows. Section II describes the model and the controller. Section III derives analytical expressions of step-to-step maps in the presence of external forces, and Section IV particularizes these results to constant and periodic force signals. Section V concludes the paper.

II. Background: Modeling and Control

This section presents an underactuated planar bipedal model—see Fig. 1—and derives a control law that generates periodic walking motions. The model and the controller can be found in [4], [16], thus the exposition here will be terse.

A. An Underactuated Planar Bipedal Robot

The biped of Fig. 1 is composed by a torso and two identical legs connected to the torso via the hip joints. Each leg is comprised of two links, the thigh and the shin, which are connected through the knee joint. The model is controlled by four actuators, two located at its hip joints and two at its knee joints. We are interested in periodic walking gaits consisting of successive phases of single support (swing phase) and double support (impact phase).

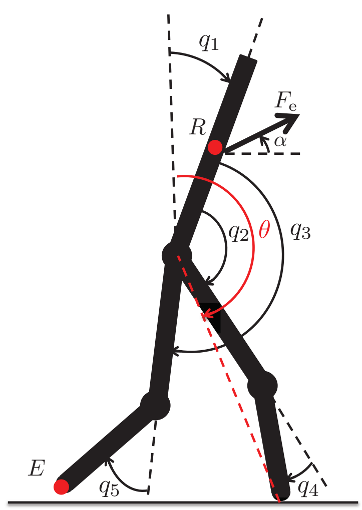

Fig. 1. Robot model with a choice of generalized coordinates.

Our objective is to characterize how periodic walking gaits are influenced by the existence of an external force $F_{\rm e}$, which acts on the system persistently, i.e., over a number of steps. To avoid technical issues and keep our development general, we will assume that the external force is a piecewise smooth function of time $F_{\rm e} : [t_0, t_{\rm f}] \to \mathbb{R}^2$, and that the interval $t_{\rm f} - t_0$ is large compared to the duration of a step.

In the single support phase, we assume that the foot in contact with the ground does not slip. The contact of the leg with the ground is modeled as an unactuated pin joint, and the model can be described by five degrees of freedom. The configuration space Q is a simply connected open subset of $[0, 2\pi)^5$ corresponding to physically reasonable configurations of the model, and is parameterized by[1] $q := (q_1, .., q_5)' \in Q$ as in Fig. 1. The dynamics of the system in the single support phase can be written as

$$D(q)\ddot{q} + C(q,\dot{q})\dot{q} + G(q) = Bu + J'(q)F_{\rm e} \ , \qquad (1)$$

where $D(q)$ is the inertia matrix, $C(q,\dot{q})\dot{q}$ contains the centrifugal and Coriolis forces and $G(q)$ the gravitational forces. The matrix B maps the input vector u containing the four actuator torques to the vector of generalized forces corresponding to q. Finally, J is the Jacobian $J(q) = \partial p_{\rm R}(q)/\partial q$, where $p_{\rm R}(q)$ is the position of the point R on the torso at which the force is applied; see Fig. 1.

Defining $x := (q', \dot{q}')'$ the model can be written as

$$\dot{x} = f(x) + g(x)u + g_{\rm e}(x)F_{\rm e} \ , \qquad (2)$$

where

$$f(x) = \begin{bmatrix} \dot{q} \\ D^{-1}(q)\big(-C(q,\dot{q})\dot{q} - G(q)\big) \end{bmatrix},$$

$$g(x) = \begin{bmatrix} 0 \\ D^{-1}(q)B \end{bmatrix}, \quad g_{\rm e}(x) = \begin{bmatrix} 0 \\ D^{-1}(q)J'(q) \end{bmatrix},$$

and $x \in TQ := \{x := (q', \dot{q}')' \mid q \in Q,\ \dot{q} \in \mathbb{R}^5\}$.

The single support phase evolves until the swing leg contacts the ground in front of the support leg, defining the switching surface $\mathcal{S}$ as

$$\mathcal{S} := \{(q', \dot{q}')' \in TQ \mid p^{\rm v}_{\rm E}(q) = 0,\ p^{\rm h}_{\rm E}(q) > 0\} \ ,$$

where $p^{\rm v}_{\rm E}$ is the height of the toe E of the swing leg and $p^{\rm h}_{\rm E}$ its horizontal distance from the support leg's toe; see Fig. 1.

In the ensuing double support phase, the swing leg impacts the ground surface and the support leg enters its swing phase. It is assumed that the double support phase is instantaneous, and that the impact of the swing leg with the ground is completely inelastic and results in no rebound or slip. Under the assumptions listed in [16, Section II-B], the double support phase can be modeled as a map $\Delta : \mathcal{S} \to TQ$ taking the final state $x^- \in \mathcal{S}$ of one swing phase to the initial state $x^+ \in TQ$ of the next, i.e.

$$x^+ = \Delta(x^-) \ .$$

The details on how to derive Δ are given in [16] and are omitted for brevity. We only mention that Δ has the form

$$\Delta(x^-) = \begin{bmatrix} \Delta_q q^- \\ \Delta_{\dot{q}}(q^-)\dot{q}^- \end{bmatrix} \ , \qquad (3)$$

where Δ_q is a constant relabeling[2] matrix and $\Delta_{\dot{q}}(q)\dot{q}$ describes the physics of the impact.

Combining the swing and impact phases, the model can be expressed in the form of a system with impulse effects as

$$\Sigma : \begin{cases} \dot{x} = f(x) + g(x)u + g_{\rm e}(x)F_{\rm e}, & x \notin \mathcal{S} \\ x^+ = \Delta(x^-), & x^- \in \mathcal{S} \end{cases} \ , \qquad (4)$$

where the symbols in (4) have the meaning explained above.

[1] Notation: To avoid cluttering, we denote the transpose of a matrix A by A' instead of the commonly used symbol $A^{\rm T}$.

[2] After impact, the swing leg becomes the new stance leg and its coordinates are relabeled.

B. HZD Controller Design

The controllers discussed in this paper are developed within the HZD framework, introduced in [16] and detailed in [4]. Effectively, controllers designed using the HZD approach achieve stable periodic walking gaits by driving a set of suitably selected output functions to zero. In more detail, to the continuous dynamics (2), associate the output

$$y = h(q) := q_{\mathrm{c}} - h_{\mathrm{des}} \circ \theta(q) \ , \tag{5}$$

where q_{c} includes the controlled variables, which are selected to be the relative angles shown in Fig. 1; i.e., $q_{\mathrm{c}} = (q_2, q_3, q_4, q_5)'$. In (5), $h_{\mathrm{des}} \circ \theta(q)$ specifies the desired evolution of q_{c}, represented as a function of the absolute angle $\theta(q) = q_1 + q_2 + \frac{1}{2}q_4$ of the line connecting the stance leg end to the hip, as shown in Fig. 1. Finally, note that a variety of ways have been proposed for designing h_{des} in (5), providing various degrees of flexibility on the desired evolution of the controlled variables; see [4], [7] for more details how h_{des} can be designed.

The objective of the controller is to drive the output (5) to zero. To achieve this, an input/output relationship is obtained by differentiating (5) twice; i.e.,

$$\ddot{y} = L_f^2 h(x) + L_g L_f h(x) u + L_{g_{\mathrm{e}}} L_f h(x) F_{\mathrm{e}} \ , \tag{6}$$

in which $L_f^2 h$, $L_g L_f h$ and $L_{g_{\mathrm{e}}} L_f h$ denote the Lie derivatives of h along the corresponding vector fields; see [4, Section B.1.5] for detailed definitions. Under the condition that the decoupling matrix $L_g L_f h$ is invertible, and assuming that the external force F_{e} is available,

$$u^*(x, F_{\mathrm{e}}) = -L_g L_f h(x)^{-1} \big[L_f^2 h(x) + L_{g_{\mathrm{e}}} L_f h(x) F_{\mathrm{e}} \big] \tag{7}$$

is the unique input that renders the zero dynamics surface

$$\mathcal{Z} := \{ x \in TQ \mid h(q) = 0, \ L_f h(x) = 0 \}$$

invariant under the flow of the swing phase dynamics. The corresponding restriction dynamics on $\mathcal{Z}$ is given by $\dot{z} = f_{\mathrm{z}}^*(z) + g_{\mathrm{e_z}}(z) F_{\mathrm{e}}$, where $f_{\mathrm{z}}^* := (f + g u^*)|_{\mathcal{Z}}$ and $g_{\mathrm{e_z}} := g_{\mathrm{e}}|_{\mathcal{Z}}$ are the restrictions on $\mathcal{Z}$ of the vector fields of the swing phase zero dynamics (2) in closed loop with (7).

If, in addition, the condition of hybrid invariance $\Delta(\mathcal{S} \cap \mathcal{Z}) \subset \mathcal{Z}$ can be ensured, then

$$\Sigma_{\mathrm{z}} : \begin{cases} \dot{z} = f_{\mathrm{z}}^*(z) + g_{\mathrm{e_z}}(z) F_{\mathrm{e}}, & z \notin \mathcal{S} \cap \mathcal{Z} \\ z^+ = \Delta_{\mathrm{z}}(z^-), & z^- \in \mathcal{S} \cap \mathcal{Z} \end{cases} \ , \tag{8}$$

where $\Delta_{\mathrm{z}} := \Delta|_{\mathcal{S} \cap \mathcal{Z}}$ is well defined and corresponds to the hybrid zero dynamics (HZD) of the model Σ defined in (4).

In practical implementations of HZD controllers, the feedback law (7) is augmented with an auxiliary control variable v so that the closed-loop input/output system (6) takes the form $\ddot{y} = v(y, \dot{y})$. A number of approaches have been suggested in the relevant literature for designing v to achieve sufficiently fast convergence to the zero dynamics surface; see for example [4] and [12] for recent results. We do not provide further details on this issue here. In what follows, we will assume that an HZD-controller that stabilizes walking by zeroing the output (sufficiently fast) is available when no external force is applied.

As a final remark, it should be emphasized that (7) requires the knowledge of the external force F_{e}. Under this assumption, the presence of F_{e} does *not* influence the closed-loop dynamics of the output. This implies that, if the system evolves on $\mathcal{Z}$ where $y = 0$ and $\dot{y} = 0$, then the presence of F_{e} does not "break" its evolution on $\mathcal{Z}$. In addition, since $\mathcal{S}$ is independent of the force, the restricted impact surface $\mathcal{S} \cap \mathcal{Z}$ also remains unaltered by the application of F_{e}. These observations will be important in Section III, where the effect of F_{e} on the stepping pattern of the biped is detailed.

III. The Effect of External Force on a Step

Our objective in this section is to examine the influence of the external force over a step and to determine conditions under which a step can be taken.

We begin with defining the restricted step map, which takes the state of (8) at the beginning of a step to the state at the beginning of the next, provided that the step is completed. To do this we first define the (restricted on $\mathcal{Z}$) time-to-impact function as follows. Suppose that the k-th step starts at $t_{k-1} \in [t_0, t_{\mathrm{f}}]$. Let $\varphi_{\mathrm{z},k}^{F_{\mathrm{e}}}(t, z_0)$ be the solution of the continuous-time part of (8) with initial condition $\varphi_{\mathrm{z},k}^{F_{\mathrm{e}}}(t_{k-1}, z_0) = z_0$. The (restricted on $\mathcal{Z}$) time-to-impact function $T_{\mathrm{I},k}^{F_{\mathrm{e}}} : \mathcal{Z} \to \mathbb{R} \cup \{\infty\}$, can then be defined as

$$T_{\mathrm{I},k}^{F_{\mathrm{e}}}(z_0) = \begin{cases} \inf \Big\{ t \in [0, +\infty) \mid \varphi_{\mathrm{z},k}^{F_{\mathrm{e}}}(t, z_0) \in \mathcal{S} \cap \mathcal{Z} \Big\}, \\ \qquad \text{if } \exists \ t \text{ such that } \varphi_{\mathrm{z},k}^{F_{\mathrm{e}}}(t, z_0) \in \mathcal{S} \cap \mathcal{Z} \\ \infty, \ \text{otherwise.} \end{cases}$$

We now proceed with the definition of the step map. Let $z^- \in \mathcal{S} \cap \mathcal{Z}$ be a pre-impact initial condition so that the post-impact state $z^+ = \Delta_{\mathrm{z}}(z^-)$ is such that $T_{\mathrm{I},k}^{F_{\mathrm{e}}}(z^+) < \infty$ for the values of the external force F_{e} over the interval $[t_{k-1}, t_k]$, where $t_k := t_{k-1} + T_{\mathrm{I},k}^{F_{\mathrm{e}}}(z^+)$. This implies that the model completes the k-th step. The corresponding step map $\rho_k : \mathcal{S} \cap \mathcal{Z} \to \mathcal{S} \cap \mathcal{Z}$ is then defined by

$$\rho_k(z^-) := \varphi_{\mathrm{z},k}^{F_{\mathrm{e}}} \big(T_{\mathrm{I},k}^{F_{\mathrm{e}}}(\Delta_{\mathrm{z}}(z^-)), \ \Delta_{\mathrm{z}}(z^-) \big) \ . \tag{9}$$

The rest of this section is devoted to the derivation of an explicit expression for the step map ρ_k, which will greatly facilitate the analysis of the effect of the external force F_{e} on the stepping pattern of the biped.

In what follows, we restrict our attention to steps for which the angle θ used to parameterize the output function (5) is a strictly monotonically increasing function of time; see Fig. 1. Intuitively, this assumption allows us to use θ to replace time in parameterizing the motion of the model, so that the output (5) is a function of the configuration variables only. Note though that requiring θ to be monotonically increasing over a step limits the walking patterns that can be achieved by the controller in the presence of the external force F_{e}.

Using now the same notation as in the definition of the step map (9), the evolution of the angle θ with respect to time over the k-th step is represented as a function $\vartheta_k : [t_{k-1}, t_k] \to \mathbb{R}$ defined by the rule $\vartheta_k(t) = \Pi \circ \varphi_{\mathrm{z},k}^{F_{\mathrm{e}}}(t, z^+)$, where the mapping Π constructs[3] θ from the flow $\varphi^{F_e}_{z,k}(t, z^+)$. Based on the discussion above, the function ϑ_k is monotonically increasing over the k-th step, and, as such, it achieves its minimum and maximum values at the end points t_{k-1} and t_k. In particular, $\vartheta_k(t_{k-1}) = \theta^+$ and $\vartheta_k(t_k) = \theta^-$, corresponding to the values of the angle θ at the beginning and the end of the k-th step, respectively.

An important observation regarding the extrema θ^- and θ^+ of ϑ_k is that they do *not* depend on the value of the external force F_e over the step, as long as the step can be completed. Intuitively, the step length does *not* change upon the application of the external force and remains equal to the one corresponding to the unforced case. This is an inherent property of the feedback controller, which reacts to the force by changing the velocity over a step. To see this, note that by [16, HH5)], there exists a unique touchdown configuration q_0^- that satisfies $(h(q_0^-), p^{\rm v}_{\rm E}(q_0^-)) = (0, 0)$. Then, q_0^+ is the post-impact configuration obtained by applying the relabeling matrix Δ_q of (3) on q_0^- which switches the role of the swing and stance legs after touchdown. The introduction of an external force does not alter $h(q)$ or $p^{\rm v}_{\rm E}(q)$; thus, q_0^- remains the same, implying that q_0^+ also remains the same over different steps. Clearly, since $\theta(q) = q_1 + q_2 + \frac{1}{2}q_4$, the extrema θ^+ and θ^- of ϑ_k do not depend on k.

Finally, note that the function ϑ_k is a bijection onto its image; that is, $\vartheta_k^{-1} : [\theta^+, \theta^-] \to [t_{k-1}, t_k]$ is well defined. We will use this fact to express the portion of the external force F_e that is acting on the biped over the duration $[t_{k-1}, t_k]$ of the k-th step as a function of the angle θ; see Fig. 2. In more detail, we define $F_k : [\theta^+, \theta^-] \to \mathbb{R}^2$ by

$$F_k(\theta) := F_e \circ \vartheta_k^{-1}(\theta) \ , \tag{10}$$

which, in general, differs among steps, as shown in Fig. 2.

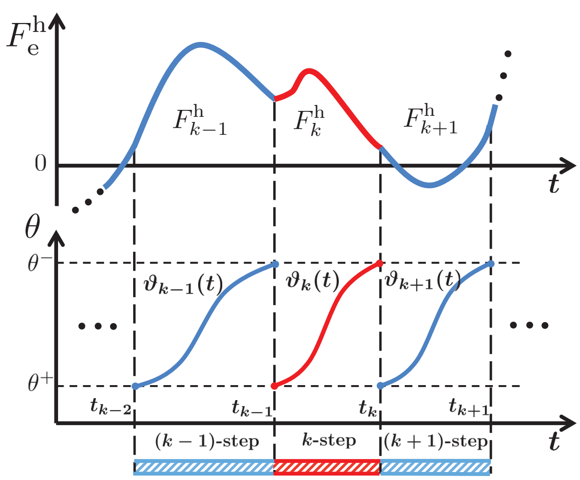

Fig. 2. Illustration of the effect of a force over a number of steps. For simplicity, a continuous force that acts in the horizontal direction is depicted.

Next we proceed with the derivation of an analytical expression for the step map ρ_k of (9) by integrating Σ_z in (8) along the k-th step. The key difference with [16] is that in our case the external force F_e needs to be taken into account. The integration can be facilitated by selecting suitable coordinates. As suggested in [16, Theorem 1],

$$\xi_1 = \theta(q), \ \xi_2 = D_1(q)\dot{q} \ , \tag{11}$$

where $D_1(q)$ denotes the first row of the mass matrix D in (1), is a valid set of coordinates on $\mathcal{Z}$.

The following lemma provides the continuous-time part of (8) expressed in the coordinates (11). Its proof is a modification of the proof of [16, Theorem 1] and is given in the Appendix.

Lemma 1: In the coordinates (11), the continuous-time part of Σ_z in (8) takes the form

$$\begin{aligned}\dot{\xi}_1 &= \kappa_1(\xi_1)\xi_2 \\ \dot{\xi}_2 &= \kappa_2(\xi_1) + \kappa_3(\xi_1)F_e \ ,\end{aligned}$$

in which

$$\begin{aligned}\kappa_1(\xi_1) &= \frac{\partial\theta}{\partial q}\begin{bmatrix}\frac{\partial h}{\partial q}\\ D_1\end{bmatrix}^{-1}\begin{bmatrix}0\\1\end{bmatrix}\Bigg|_{\mathcal{Z}} \ , \\ \kappa_2(\xi_1) &= -\,G_1|_{\mathcal{Z}} \ , \\ \kappa_3(\xi_1) &= J_1'|_{\mathcal{Z}} \ ,\end{aligned}$$

where G_1 and J_1' are the first rows of G and J' respectively.

In the coordinates of Lemma 1, the continuous part of (8) can be integrated as follows. Let $\zeta := \frac{1}{2}(\xi_2)^2$ be an auxiliary variable so that

$$\frac{d\zeta}{d\xi_1} = \frac{\kappa_2(\xi_1) + \kappa_3(\xi_1)F_e(\vartheta_k^{-1}(\xi_1))}{\kappa_1(\xi_1)} \ , \tag{12}$$

Then, integrating (12) over the k-th step results in

$$\zeta^-[k] = \zeta^+[k] - V(\theta^-) + W_k(\theta^-). \tag{13}$$

in which ζ^+ and ζ^- are the post- and pre-impact values of ζ and V and W_k are given by

$$V(\xi_1) := -\int_{\theta^+}^{\xi_1} \frac{\kappa_2(\xi)}{\kappa_1(\xi)} d\xi \tag{14}$$

$$W_k(\xi_1) := \int_{\theta^+}^{\xi_1} \frac{1}{\kappa_1(\xi)} \left(\kappa_3(\xi)F_k(\xi)\right) d\xi \ , \tag{15}$$

where F_k corresponds to the part of the force F_e that is acting on the biped over the k-th step expressed as in (10). Notice that the index k appears explicitly as a subscript of W_k to emphasize that these functions may differ among steps due to the possibly varying force; see Fig. 2. On the other hand, the function V is independent of the force and it does not change among different steps.

To complete the derivation of the step map ρ_k, the discrete part of the system Σ_z in (8) is taken into account. The following lemma gives the form of Δ_z in (8) in the coordinates (11); its proof is a direct consequence of the arguments in [16, Section IV-A] and is omitted.

Lemma 2: In the coordinates (11), the discrete part of Σ_z in (8) takes the form

$$\Delta_z(z^-) = [\theta^+ \quad \delta_z \xi_2^-]'$$

where δ_z is a *constant* computed as in [16, Section IV-A].

[3] In the coordinates (11), $\Pi := [1 \ 0]$ projecting the flow $\varphi^{F_e}_{z,k}(t, z^+)$ to its first component.

With the help of Lemma 2, the post-impact value $\zeta^+[k]$ in (13) can be computed as $\zeta^+[k] = \delta_{\rm z}^2 \zeta^-[k-1]$ so that

$$\zeta^-[k] = \rho_k(\zeta^-[k-1]) \ , \tag{16}$$

where

$$\rho_k(\zeta^-) := \delta_{\rm z}^2 \zeta^- - \big[V(\theta^-) - W_k(\theta^-)\big] \tag{17}$$

represents the step map of the k-th step expressed as a function of the pre-impact value ζ^- of ζ.

A number of interesting observations can be made, owing to the availability of the explicit form (17) for the step map (16). First, note that the coefficient $\delta_{\rm z}$ does *not* depend on the step number k. As was mentioned above, the same is true for the function V given by (14). Then, as k varies, ρ_k defined by (17) represents a family of affine functions each having the same slope $\delta_{\rm z}^2$ but different offsets, which depend on the force and capture its effect on the system.

Furthermore, the domain of definition of ρ_k associated with the k-th step can be characterized explicitly as

$$\mathcal{D}_k = \big\{\zeta^- > 0 \mid \delta_{\rm z}^2 \zeta^- - M_k \geq 0\big\} \tag{18}$$

where

$$M_k := \max_{\theta^+ \leq \xi_1 \leq \theta^-} \left[V(\xi_1) - W_k(\xi_1)\right] \ .$$

This implies that if $\zeta^- \in \mathcal{D}_k$ the biped takes a well-defined step. Note that this step may not be one that repeats itself, as is the case for periodic walking gaits, such as those typically computed in the absence of an external force. In fact, aperiodic motions—i.e., motions in which each step is different—can be realized depending on the form of the external force $F_{\rm e}$; see Section IV-B. Yet, as long as $\zeta^-[k-1] \in \mathcal{D}_k$, the biped will take the k-th step.

To further understand how the biped reacts to the application of an external force, we discuss the effect of such force on the velocity of the system over the k-th step, provided that the initial condition $\zeta^-[k-1] \in \mathcal{D}_k$ so that the step can be completed. If the force $F_k(\theta)$ is known, a (forced) fixed point of the k-th step map ρ_k can be computed by

$$\zeta_k^* = -\frac{V(\theta^-) - W_k(\theta^-)}{1 - \delta_{\rm z}^2} \ , \tag{19}$$

and is exponentially stable if, and only if, $\delta_{\rm z}^2 < 1$, which corresponds to the fraction of kinetic energy lost at impact. Due to the exponential stability of ζ_k^*, the initial condition $\zeta^-[k-1]$ of the step will be attracted by ζ_k^*. Hence, if $\zeta^-[k-1] < \zeta_k^*$, the biped will take a faster step to catch up with the fixed ζ_k^*, while if $\zeta^-[k-1] > \zeta_k^*$ the biped will take a slower step to approach ζ_k^*. It should be noted that the fixed point ζ_k^* may *never* be realized despite its exponentially stable nature because the maps ρ_k generally vary from one step to the next in a fashion that depends on the external force.

Finally, it is of interest to describe how the proposed HZD controller takes advantage of the underactuated nature of the robot to respond to the externally applied force. Intuitively, the controller organizes the closed-loop biped so that its evolution is governed by the absolute angle θ, which, due to the one degree of underactuation of the system, remains uncontrolled. The external force then interacts with θ in a way that accelerates or decelerates the biped depending on the direction along which $F_{\rm e}$ acts.

IV. Examples of Forcing Patterns

To provide further insight, this section considers concrete examples of externally applied forces. We assume that an exponentially stable limit cycle corresponding to a periodic walking motion in the absence of external forcing is available. Such motion is associated with a fixed point

$$\zeta_0^* = -\frac{V(\theta^-)}{1 - \delta_{\rm z}^2} \ , \tag{20}$$

of the map (17), which in the absence of a force becomes

$$\rho_0(\zeta^-) := \delta_{\rm z}^2 \zeta^- - V(\theta^-) \ ,$$

with domain of definition

$$\mathcal{D}_0 = \big\{\zeta^- > 0 \mid \delta_{\rm z}^2 \zeta^- - M_0 \geq 0\big\}$$

where $M_0 := \max_{\theta^+ \leq \xi_1 \leq \theta^-} V(\xi_1)$. Exponential stability is ensured by the condition $\delta_{\rm z}^2 < 1$. Note that in (20), the subscript "0" is used to denote zero external force. Walking motions of this type can be realized via a straightforward application of the methods described in [4]. In this section, we use the results of Section III to discuss how such unforced motions "adapt" to an externally applied force.

A. Constant External Force

We begin with the case of a constant external force, i.e., $F_{\rm e}(t) \equiv F\hat{\rm r}$, where $\hat{\rm r} \in \mathbb{R}^{2\times 1}$ is the (constant) unit vector along the direction of the force, and F is a constant for all $t \in [t_0, t_{\rm f}]$. Applying a constant external force provides clear interpretations of the adaptability of periodic walking motions to external forcing.

In the case of a constant force, the subscripts k denoting step number can be dropped since the effect of a constant force is the same over all steps. With this convention, the step map defined by (17) will be denoted by ρ and its domain of definition, which is characterized by (18) with $M := \max_{\theta^+ \leq \xi_1 \leq \theta^-} [V(\xi_1) - W(\xi_1)]$, where

$$W(\xi_1) := F \int_{\theta^+}^{\xi_1} \frac{1}{\kappa_1(\xi)} \left(\kappa_3(\xi)\hat{\rm r}\right) d\xi \ ,$$

will be denoted by $\mathcal{D}$. A fixed point ζ^* of (17), when it exists, can be computed by (19).

Suppose now that the force acts along the direction of motion. In this case, the inner product $\kappa_3(\xi)\hat{\rm r} > 0$; see Lemma 1 for the interpretation of κ_3. Then, if $\kappa_1(\xi) > 0$, which can be verified in simulation, we have that $W(\theta^-) > 0$, and hence $M < M_0$ implying that the lower bound of the domain of definition decreases. Furthermore, because the function V and the constant $\delta_{\rm z}$ do *not* depend on the external force, from (19) and (20) one can show that

$$\zeta^* = \zeta_0^* + \frac{W(\theta^-)}{1 - \delta_{\rm z}^2} \ ,$$

which implies $\zeta^* > \zeta_0^*$. Intuitively, this fact means that, in response to an external force that is applied along the

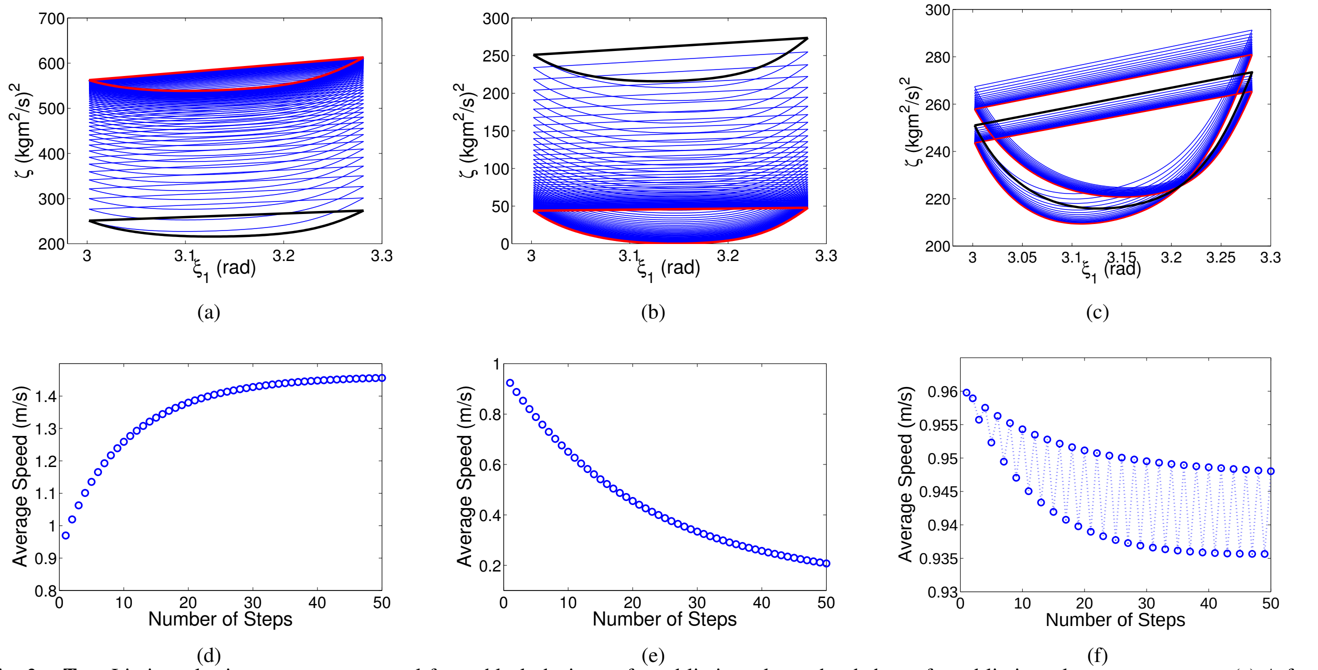

Fig. 3. **Top:** Limit cycles in response to external force; black depicts unforced limit cycles and red shows forced limit cycles at convergence. (a) A force $(5, 0)'$N acts in the direction of the unforced motion. (b) A force $(-3.32, 0)'$N opposes the unforced motion. (c) A periodic force $(5\sin(\frac{2\pi}{0.47}t), 0)'$N is applied. **Bottom:** Average speed as the system converges to a forced limit cycle. (d) Convergence to higher speed in response to the force of (a). (e) Convergence to lower speed in response to the force of (b). (f) Convergence to a two-step periodic motion at lower speed in response to the force of (c).

direction of the motion, the biped will take faster steps and eventually converge to a new fixed point that is at higher velocity than the one corresponding to the unforced case.

Suppose next that the external force opposes the unforced motion, so that $\kappa_3(\xi)\hat{\mathrm{r}} < 0$. Based on similar arguments as above, one can deduce that $M > M_0$ implying that the lower bound of the domain of definition increases. This is different from the situation where the external force "pulls" the system in the direction that is already moving. As a result, stricter conditions on *both* the external force and the unforced limit cycle must be satisfied for the robot to converge to a forced periodic motion. In more detail, a forced fixed point exists if the solution of $\zeta^- = \rho(\zeta^-)$ is in the domain of definition $\mathcal{D}$ of ρ. Using (19) and (18), this condition takes the form

$$\zeta_0^* \geq -\frac{1}{1-\delta_{\mathrm{z}}^2} W(\theta^-) + \frac{1}{\delta_{\mathrm{z}}^2} M \quad , \tag{21}$$

in which the meaning of ζ_0^*, $W(\theta^-)$ and M is the same as above. The inequality (21) couples the effect of both the unforced motion ζ_0^* and of the external force, and, if it is satisfied, the biped converges to a forced limit cycle ζ^*. Using similar arguments as above, one can show that the resulting forced motion is at a lower speed than the original unforced one, owing to the fact the force resists the unforced motion of the system.

In summary, the application of an external force in the direction of the motion will push the system to take faster steps, so that it eventually converges to a forced fixed point. On the other hand, when the external force resists the unforced motion, whether the system converges to a new periodic motion depends on the unforced fixed point and on the force applied in a way that is captured by (21). It is worth noting that removing the external force will cause the system to converge back to its original (unforced) motion.

Finally, Figs. 3(a) and 3(b) show convergence to a forced limit cycle upon the application of a constant external force; Fig. 3(a) shows an example in which the force acts in the same direction as the direction of the unforced motion and Fig. 3(b) an example of the opposite case. Figures 3(d) and 3(e) show the corresponding evolution of the velocity as a function of the step, where it is seen that the number of steps required until convergence is larger in the case where force opposes the motion. Note that in all these results the corresponding ground interaction constraints are satisfied.

B. Periodic External Forces

The availability of explicit expressions for the step map in Section III facilitates the analysis of how a more general class of external forcing signals affects periodic walking motions. For brevity, we do not provide detailed discussions here; rather, we focus on providing some intuition on how the biped reacts to such external signals.

In the case where a (piecewise smooth) force $F_{\mathrm{e}}(t)$ with period T_{F} is applied over the interval $[t_0, t_{\mathrm{f}}]$, an explicit condition that ensures that the biped will keep taking steps can be derived. Let $F := \max_{t\in[t_0,t_{\mathrm{f}}]} \|F_{\mathrm{e}}(t)\|_2$ and $\hat{\mathrm{r}}(\xi_1)$ be the unit vector along the direction defined by κ_3. Then, the robot will continue to take steps if

$$\zeta_0^* \geq -\frac{1}{1-\delta_{\mathrm{z}}^2} \tilde{W}(\theta^-) + \frac{1}{\delta_{\mathrm{z}}^2} M \quad , \tag{22}$$

where

$$\tilde{W}(\xi_1) := -F\int_{\theta^+}^{\xi_1} \frac{1}{\kappa_1(\xi)} \kappa_3(\xi)\hat{r}(\xi) d\xi$$

and $M = \max_{\theta^+ \leq \xi_1 \leq \theta^-}[V(\xi_1) - \tilde{W}(\xi_1)]$. Note that this condition is conservative since it takes into account the worst possible forcing situation. A more refined condition can be stated, but we do not provide it here as it requires a recursive expression over the number of steps. Nevertheless, it is useful to know that a condition that couples the underlying unforced motion ζ_0^* with the external force through the constants M and $\tilde{W}(\theta^-)$ can be stated explicitly.

As long as (22) is satisfied, the biped will keep taking steps. However, whether it will eventually converge to a periodic gait depends on the period $T_{\rm F}$ of the force. It was observed in simulations that if $T_{\rm F}$ is a rational number, then the system always converges to a forced periodic gait. Furthermore, one can prove that if the biped converges to such limit cycle, then the corresponding motion is composed by $K \in \mathbb{Z}_+$ steps and its period is an integer multiple of the period of the force; i.e., there exists $N \in \mathbb{Z}_+$ so that

$$\sum_{k=1}^{K}[t_k - t_{k-1}] = NT_F \ . \tag{23}$$

To demonstrate these observations, Fig. 3(c) presents an example of a two-step limit cycle that was generated by applying a periodic force on the biped while it was following an unforced periodic walking gait. As can be seen in Fig. 3(f), the biped converges to a periodic gait in which a fast step is followed by a slow step, and the total duration of the cycle is equal to the period of the external force confirming (23). As a final remark, in the case where the external force is almost periodic or aperiodic, the biped will keep taking steps as long as the condition (22) is satisfied.

V. Conclusion

This paper studied the ability of an underactuated bipedal robot model to adapt to external forces. Our analysis begins with periodic walking gaits that are computed in the absence of the external force using the HZD method. Upon application of a force, it was shown that the biped modifies its (unforced) stepping pattern to one that is consistent with the external force, provided that certain (analytically available) conditions that couple the externally applied force and the unforced motion are satisfied. Concrete examples of forcing patterns corresponding to forces that are constant or periodic have also been discussed. It turns out that the interaction between the feedback controller used and the underactuated nature of the biped governs the adaptability of its motion to external forces. This work represents a first step toward controllers that treat the environment within which a biped operates not as a source of disturbances that need to be rejected, but rather as a source of "commands" to which the robot needs to adapt.

Appendix

Proof: [Lemma 1] The derivation of κ_1 is in [16, Theorem 1]. To obtain κ_2, κ_3, define $\gamma(x) := D_1(q)\dot{q}$ so that $\xi_2 = \gamma(x)$ and $L_g\gamma = 0$ as in [16]. Then, $\dot{\xi}_2$ is

$$\begin{aligned} \dot{\xi}_2 &= L_f\gamma(x) + L_{g_{\rm e}}\gamma(x)F_{\rm e} \\ &= \begin{bmatrix} \dot{q}'\frac{\partial D_1'(q)}{\partial q} & D_1(q) \end{bmatrix} \left(\begin{bmatrix} \dot{q} \\ D^{-1}(q)[-C(q,\dot{q})\dot{q} - G(q)] \end{bmatrix} \right. \\ &\quad \left. + \begin{bmatrix} 0 \\ D^{-1}(q)[J'(q)F_e] \end{bmatrix} \right) \ . \end{aligned} \tag{24}$$

Then, use $C_1(q,\dot{q}) = \dot{q}'\frac{\partial D_1'(q)}{\partial q} - \frac{1}{2}\dot{q}'\frac{\partial D(q)}{\partial q_1}$ and $\partial D(q)/\partial q_1 = 0$ as in the proof of [16, Theorem 1] in (24) to obtain $\dot{\xi}_2 = -G_1(q) + J_1'(q)F_e$, which results in the expressions for κ_2 and κ_3 by taking restrictions on $\mathcal{Z}$ so that they become functions of ξ_1. ■

References

[1] B. Stephens, "Push Recovery Control for Force-Controlled Humanoid Robots," Ph.D. dissertation, Carnegie Mellon University, 2011.

[2] H. Diedam, D. Dimitrov, P.-B. Wieber, K. Mombaur, and M. Diehl, "Online walking gait generation with adaptive foot positioning through linear model predictive control," in *Proceedings of IEEE/RSJ International Conference on Intelligent Robots and Systems*, Nice, France, September 2008, pp. 1121–1126.

[3] K. Harada, E. Yoshida, and K. Yokoi, Eds., *Motion planning for humanoid robots*. Springer-Verlag, 2010.

[4] E. R. Westervelt, J. W. Grizzle, C. Chevallereau, J. H. Choi, and B. Morris, *Feedback Control of Dynamic Bipedal Robot Locomotion*. Boca Raton, FL: CRC Press, 2007.

[5] A. Ames, K. Galloway, J. Grizzle, and K. Sreenath, "Rapidly exponentially stabilizing control lyapunov functions and hybrid zero dynamics," *IEEE Transactions on Automatic Control*, vol. 59, no. 4, pp. 876–891, 2014.

[6] K. A. Hamed and J. W. Grizzle, "Event-based stabilization of periodic orbits for underactuated 3-D bipedal robots with left-right symmetry," *IEEE Transactions on Robotics*, vol. 30, no. 2, pp. 365–381, 2014.

[7] K. Sreenath, H. Park, I. Poulakakis, and J. Grizzle, "A compliant hybrid zero dynamics controller for stable, efficient and fast bipedal walking on MABEL," *International Journal of Robotics Research*, vol. 30, no. 9, pp. 1170–1193, 2011.

[8] A. E. Martin, D. C. Post, and J. P. Schmiedeler, "The effects of foot geometric properties on the gait of planar bipeds walking under HZD-based control," *International Journal of Robotics Research*, vol. 33, no. 12, pp. 1530–1543, 2014.

[9] A. D. Ames, "Human-inspired control of bipedal walking robots," *IEEE Transactions on Automatic Control*, vol. 59, no. 5, pp. 1115–1130, May 2014.

[10] R. Gregg and M. Spong, "Reduction-based control of three-dimensional bipedal walking robots," *International Journal of Robotics Research*, vol. 2010, no. 6, pp. 680–702, 26.

[11] C. O. Saglam and K. Byl, "Robust policies via meshing for metastable rough terrain walking," in *Robotics 2014: Science and Systems*, 2014.

[12] A. D. Ames and M. Powell, "Towards the unification of locomotion and manipulation through control lyapunov functions and quadratic programs," in *Control of Cyber-Physical Systems, Lecture Notes in Control and Information Sciences*. Springer, 2013, pp. 219–240.

[13] P.-Y. Oudeyer, O. Ly, and P. Rouanet, "Exploring robust, intuitive and emergent physical human-robot interaction with the humanoid acroban," in *Proceedings of the IEEE-RAS International Conference on Humanoid Robots*, Bled, Slovenia, Oct. 2011, pp. 120–127.

[14] M. S. Motahar, S. Veer, J. Huang, and I. Poulakakis, "Integrating dynamic walking and arm impedance control for cooperative transportation," in *Proceedings of IEEE International Conference on Intelligent Robots and Systems*, Hamburg, Germany, September/October 2015.

[15] J. Pratt, J. Carff, S. Drakunov, and A. Goswami, "Capture point: A step toward humanoid push recovery," in *Proceedings of IEEE-RAS International Conference on Humanoid Robots*, Genoa, Italy, December 2006, pp. 200–207.

[16] E. R. Westervelt, J. W. Grizzle, and D. E. Koditschek, "Hybrid zero dynamics of planar biped walkers," *IEEE Transactions on Automatic Control*, vol. 48, no. 1, pp. 42–56, 2003.